Electronic Supporting Information

A novel hafnium-graphite oxide catalyst for Meerwein-Ponndorf-Verley reaction and the activation effect of the solvent

Xiaomin Li[a], Zhengjiang Du[a], Yi Wu[a], Yadong Zhen[a], Rixin Shao[a], Bingqi Li[a], Chengmeng Chen[b], Quansheng Liu[a], Huacong Zhou[a]*

[a] College of Chemical Engineering, Inner Mongolia University of Technology; Inner Mongolia Key Laboratory of High-Value Functional Utilization of Low Rank Carbon Resources, Hohhot 010051, Inner Mongolia, China

[b] CAS Key Laboratory of Carbon Materials, Institute of Coal Chemistry, Chinese Academy of Sciences.

*Corresponding author. Email address: hczhou@imut.edu.cn (H. Zhou)

Contents

S1. Catalyst characterization

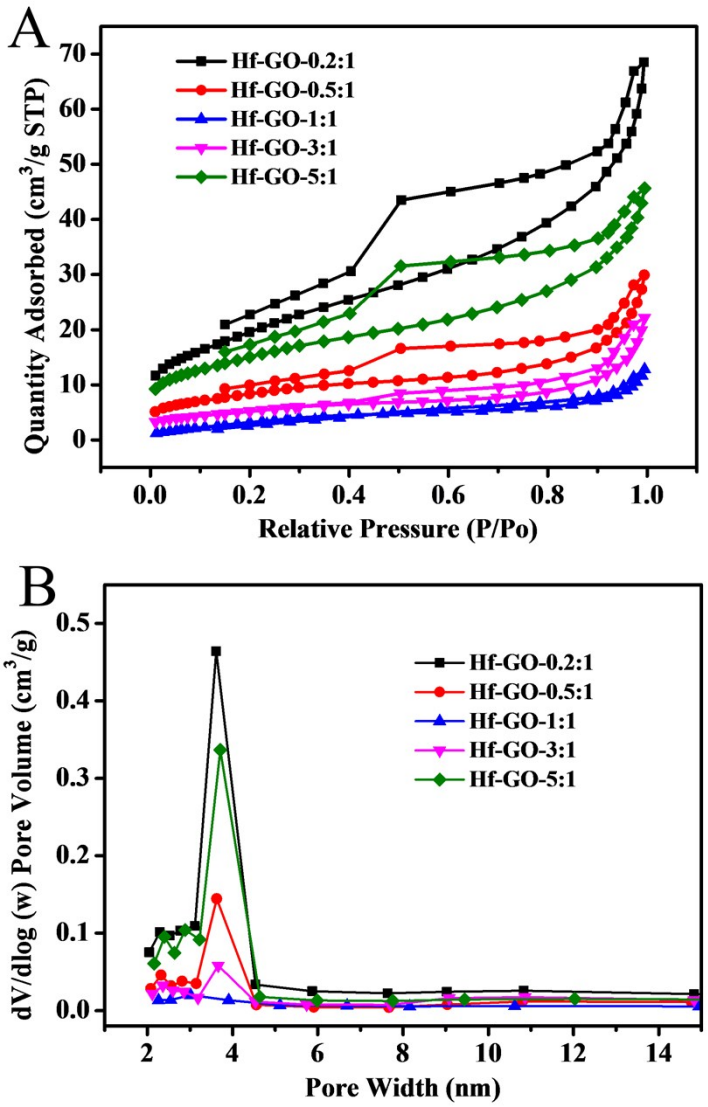

Fig. S1. N_2 adsorption-desorption isotherms (A) and pore size distributions (B) of the Hf-GO catalysts prepared with different mass ratios of Hf precursor to GO. The pore size distribution was calculated based on the DFT method.

Table S1. Comparison of structures of GO and Hf-GO catalysts with different mass ratios of Hf precursor and GO.

Sample	S_{BET} (m^2/g)[a]	V_t (cm^3/g)[b]	V_{mic} (cm^3/g)[b]	V_{mes} (cm^3/g)[b]	D_{mea} (nm)[c]	Hf (wt%)[d]
GO	98.8	0.13	0.02	0.11	4.6	-
Hf-GO-0.2:1	71.5	0.11	0.01	0.10	4.7	6.64
Hf-GO-0.5:1	30.1	0.05	0.01	0.04	5.6	10.01
Hf-GO-1:1	14.1	0.02	0.004	0.016	7.2	12.03
Hf-GO-3:1	18.9	0.04	0.01	0.03	7.0	11.95
Hf-GO-5:1	54.2	0.07	0.01	0.06	4.4	12.47

[a] S_{BET}: Brunauer-Emmett-Teller (BET) specific surface area.

[b] Volume of pores was estimated from single point adsorption total pore volume of pores.

[c] D_{mea}: average pore size was estimated from the BJH desorption average pore diameter.

[d] Measurements by Inductively coupled plasma atomic emission spectroscopy (ICP-AES).

Table S2. Effect of different modulators used during Hf-GO preparation on the conversion of EL to GVL[a].

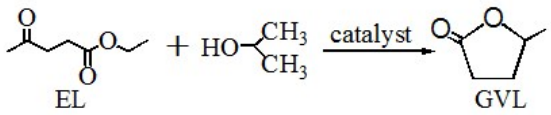

modulator	Molar ratio of modulator to Hf	EL conv.(%)	GVL yield(%)	GVL sel.(%)
None	-	59.4	51.7	87.1
AA [b]	21	49.8	43.6	87.5
BA [c]	21	59.2	45.1	76.2
FA [d]	21	82.0	76.7	93.5
TFA[e]	21	54.2	43.4	80.2
HCl [f]	21	48.5	35.8	73.8

[a] Preparation condition: 33.55 mmol modulator was dissolved in DMF (400 mL), 0.5 g $HfCl_4$ was added into DMF solution with continuously stirred and completely dissolved. After that, 1.0 g of GO was directly added to the $HfCl_4$ solution and the obtained mixture was stirred for 3 h at 30 °C, then aged at 80 °C under static conditions for 3 h. The suspended solution was separated by filtration to give black precipitate, and successively washed with DMF, ethanol for 4 times, dried under vacuum conditions at 80 °C for 24 h, and crowded into powders. Reaction conditions: 1 mmol EL, 0.1 g catalyst, 5 mL 2-PrOH , reaction temperature 150 °C, and reaction time 3 h.

[b] Acetic acid. [c] Benzoic acid. [d] Formic acid. [e] Trifluoroacetate. [f] Concentrated hydrochloric acid

The as-obtained Hf-GO was characterized in detail. The as-obtained Hf-GO was characterized by SEM, TEM, SEM-EDS, XRD, BET, TG, FTIR, Raman and XPS. SEM and TEM were employed to characterize the microscopic morphology of the obtained catalyst (Fig. 2A and B). It can be observed that the catalyst surface exhibited crumpled sheets. EDS result gave a strong Hf signal in the catalyst which indicated the Hf element was successfully introduced into GO (Fig. S3A). EDS mappings confirmed the homogeneous distribution of Hf (Fig. 2C and D).

The FTIR spectrum of GO and Hf-GO catalyst in Fig. 2E exhibited the asymmetric (GO, 1731 cm^{-1}; Hf-GO, 1723 cm^{-1}) and symmetric (GO, 1616 cm^{-1}; Hf-GO, 1655 cm^{-1}) stretching vibration of carboxylate groups. FTIR showed that the wavenumber difference of the asymmetric and symmetric vibrations of carboxylate anions was narrowed from 115 cm^{-1} for GO to 68 cm^{-1} for Hf-GO, indicating that Hf^{4+} was coordinated with carboxylate groups [1-3]. It has reported the bands at around 520 and 760 cm^{-1} were characteristic of Hf-O bonds [4], and herein the catalyst had an absorption band at 690 cm^{-1} assigned to Hf-O vibration compared with the FTIR spectrum of GO, further verifying the carboxylate groups were coordinated to Hf^{4+} ions. The bands at 1731 cm^{-1} and 1616 cm^{-1} are due to C=O stretching vibration of carbonyl and C-O stretching vibration in the COOH group, whereas the peak positions at 2800~2980 cm^{-1}, 1241 cm^{-1} and 1060 cm^{-1} ascribed to CH_3 or CH_2, C-O-C and C-OH groups stretching vibration, respectively [5, 6]. The bands at 3500-3000 cm^{-1} and 1400 cm^{-1} can be attributed to the characteristic stretching vibrations of hydroxyl and bending vibration of water molecules, respectively, which might also be

contributed to the carboxyl groups of GO moieties which were incompletely coordinated with Hf [7, 8]. Additionally, Hf-GO was found to exhibit distinct band at 1424 cm^{-1} corresponding to the stretching vibration of C-N group [9]. Due to only one component containing N element was used during the catalyst preparation, i.e., DMF, and thus the N element in the catalyst could be attributed to the residual DMF in the catalyst.

X-ray diffraction (XRD) demonstrated that Hf-GO had low crystallinity. Fig. 2F shows the XRD patterns of graphite oxide displayed characteristic peak of (001) at 2θ=12º, having a *c*-axis interlayer spacing of 0.74 nm (Table S3). It was due to the presence of oxygen functionality after oxidation of graphite. The peaks of (002) at 2θ=21º (d=0.42 nm) and (010) at 2θ=42º (d=0.21 nm) were the original graphite peaks, which were consistent with the reported results [5, 10]. The Hf-GO catalyst gave a weak diffraction peak at 2θ=10º (d=0.80 nm) and a main broad peak at 2θ=21º, which was most likely due to that the introduction of Hf^{4+} led to structural modification of GO molecules and the interlayer distance of GO layers being held apart by Hf. Thus the intensity of (001) peaks decreased and interlayer spacing upward, and the intensity increasing of (002) peaks was resulted from the poorer crystallinity, indicating an amorphous structure of Hf-GO [1, 2, 11, 12].

The Raman spectra (Fig. S2) of GO and Hf-GO catalyst had two peaks between 1200 cm^{-1} and 1800 cm^{-1}. The D band at 1350 cm^{-1} was appointed to a breathing mode of *k*-point phonons of A_{1g} symmetry ascribed to local defects and disordered structures of the inter-layer of GO and the edge of the carbon sheets. The G band at

near 1380 cm^{-1} was often appointed to the E_{2g} symmetry of the sp^2 bond of carbon atoms [13-17]. The peak for Hf-GO catalyst at G band was down shifted to 1589 cm^{-1} and D band was up shifted to 1350 cm^{-1} as compared to GO (1596 cm^{-1}, 1345 cm^{-1}). Furthermore, the slightly increased intensity ratio of I_D/I_G from 0.94 to 1.00 (Table S4) after assembly was identified as indication of the successful covalent functionalization of Hf^{4+} with COOH of GO .

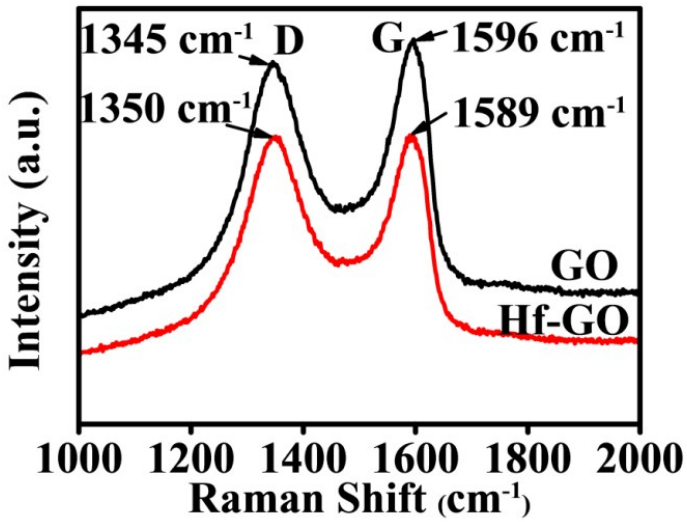

Fig. S2. Raman spectra of Hf-GO and GO.

N_2 adsorption-desorption isotherms gave reversible type IV for GO and Hf-GO, which was one of the main characteristics of mesoporous materials (Fig. S3C). The BET surface area, pore volume, and average pore size for GO were 98.8 $m^2 g^{-1}$, 0.13 $cm^3 g^{-1}$, and 4.6 nm, respectively. The above three values for Hf-GO were 61.8 $m^2 g^{-1}$, 0.08 $cm^3 g^{-1}$, and 6.1 nm, respectively. The thermal stability of Hf-GO and GO is shown in Fig. S3D. The large weight loss could be attributed to the decomposition of oxygen functional groups present in GO occurring under the temperature around 200 °C (120-300 °C) [5, 14]. The weight loss in the 300-500 °C temperature range was

ascribed to the organic-to-inorganic conversion with the release of volatile gases [4, 9]. When the temperatures were above 500 °C, less weight loss for Hf-GO was observed compared to GO. These results proved that the good stability of Hf-GO.

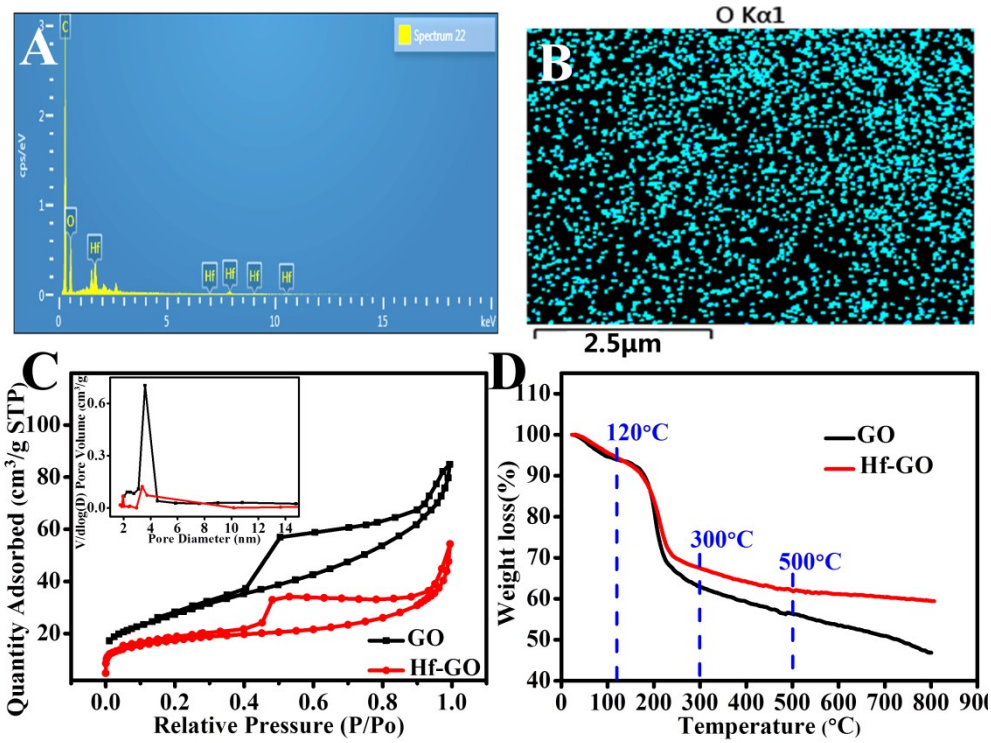

Fig. S3. (A) EDS, (B) EDS mapping of Hf-GO, (C) N_2 adsorption-desorption isotherms, and (D) TG curves of Hf-GO and GO.

S2. Effect of the Hf-GO dosage on transfer hydrogenation

The effect of the Hf-GO dosage on the reaction of EL to GVL was investigated with isopropanol as the hydrogen source at 150 °C with a reaction time of 3 h (Fig. S4A). As expected, the conversion of EL and the GVL yield increased with the rising Hf-GO dosage, and a moderate GVL yield of 40.8 % and selectivity of 73.3% were obtained even under a low catalyst amount (0.01g Hf-GO, 0.5 mol% Hf),

demonstrating the high efficiency of the catalyst. Obviously maximum conversion of EL (82.0 %) and GVL yield of 76.7 % was achieved at 150 °C under 0.1 g Hf-GO dosage (5 mol% Hf). And after the catalyst amount was increased to 0.15g (7.5 mol% Hf), the conversion improved sluggishly but the yield had a downward trend, which might be due to the product adsorption on the catalyst during sample post-treatment after reaction due to the large volume of the catalyst under high dosage. Thence, the optimal dosage of 0.1 g Hf-GO catalyst in this work was used in the subsequent experiments.

S3. Effect of reaction temperature and time on transfer hydrogenation

The effect of the reaction temperature and time on transfer hydrogenation was investigated with isopropanol as the hydrogen source. Clearly, the reaction temperature and time had a significant effect on the hydrogenation reaction. The conversion of EL and the yield of GVL gradually increased with the temperature increasing from 130 °C to 170 °C (Fig. S4B), which indicated that high temperature was conducive for the reaction of EL to GVL. The conversion of EL and the GVL yield could reach 75.8 % and 68.3 % within 3 h at 150 °C. After 150 °C, both conversion and yield increased at a slower rate, and the selectivity was nearly independent of reaction temperature. Hence, taking into account the reaction rate, we chose the medium temperature of 150 °C was the optimal reaction temperature. It was shown in Fig. S4C that the conversion of EL and the yield and selectivity of GVL increased faster with increasing the reaction time from 0 to 3 h, and the reaction proceeded slowly by prolonging the reaction time. Finally, 96.5 % conversion of EL

and 88.8 % yield of GVL could be reached within 9 h at 150 °C.

S4. Leaching of the Hf-GO catalyst

The heterogeneity of the catalyst was important for evaluating the value of a catalyst. The leaching experiment was carried out and shown in Fig. S4D. In the experiment, the solution was continued reacting at 150 °C for 9 h by removing the solid catalyst from the reaction mixture after the reaction was conducted for 1.5 h. The results were compared with the reaction that Hf-GO existed among the whole reaction duration to see if the GVL yield further increased in the absence of the Hf-GO catalyst. Obviously, the yield of GVL was no further increase after filtering out Hf-GO, indicating that the active species leaching into the reaction mixture was negligible and the Hf-GO was heterogeneous in the catalytic process.

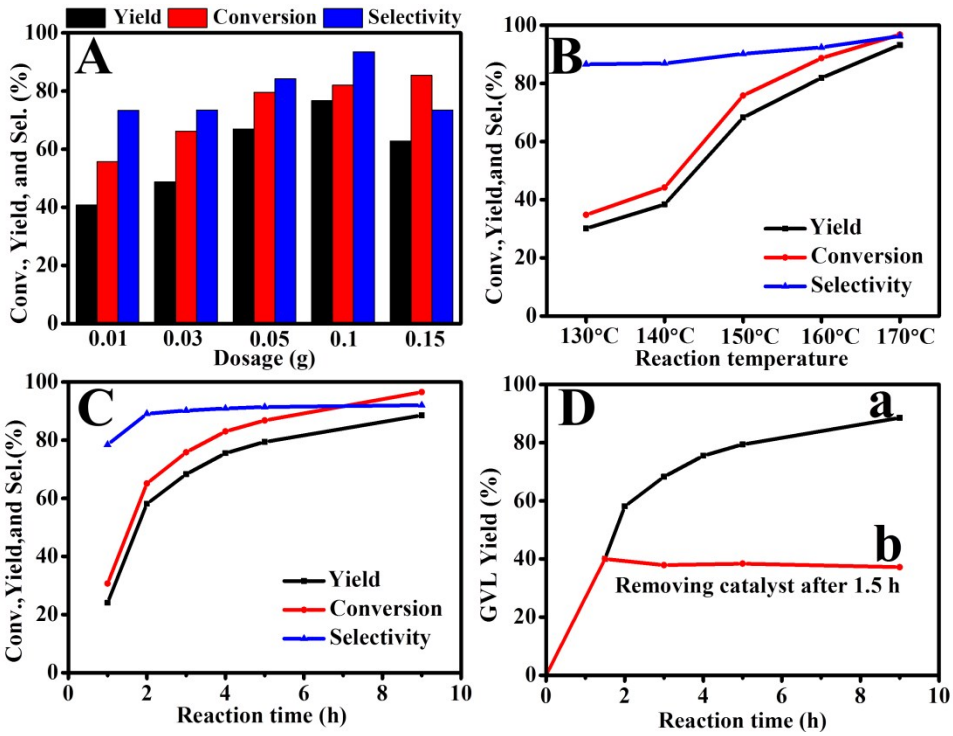

Fig. S4. Effect of the Hf-GO dosage (A), reaction temperature (B), reaction time (C) heterogeneity (D) on the conversion of EL to GVL, and (D) heterogeneity of Hf-GO. Preparation condition: stirred for 3 h at 30 °C and then aged under static conditions at 80 °C for 3h, mass ratio Hf:GO=0.5:1, molar ratio of formic acid to Hf is 21:1, solvent DMF. Reaction conditions: (A) 1.0 mmol EL, 5 mL isopropanol, 150 °C, 3.0 h. (B) 1 mmol EL, 0.1 g catalyst, 5 mL 2-PrOH, the required reaction temperature, and reaction time 3 h. (C), (D) 1 mmol EL, 0.1 g catalyst, 5 mL 2-PrOH, reaction temperature 150 °C, and the required reaction time.

S5. Recycle of the Hf-GO catalyst

The catalyst recycling was performed under the optimal reaction conditions of 0.1 g catalyst at 150 °C and 2 h. The repeated catalytic performance on the conversion of EL to GVL was displayed in Fig. 4. Inconceivably, compared with the first run, the catalytic activity did not decline but increase noticeably, i.e., the conversion of EL

and GVL yield in the second run enhancing to 88.1% and 83.8%, which was around 25% higher than those of the first run (65.1% EL conversion and 58.1% GVL yield). It was deduced that the catalyst was possibly activated after participating in the first reaction. Besides, EL conversion and GVL yield only slightly decreased after ten repeated runs between the second and eleventh (72.7% EL conversion and 66.9% GVL yield). We speculated that it might be caused by the mass loss of the catalyst after each recycle. Consequently, the Hf-GO catalyst recovered after eleven cycles was dried, weighed and replenished to the initial mass, and then reused in the twelfth run under the same conditions. The results showed that EL conversion and GVL yield in the twelfth run were enhanced to 78.2% and 72.7%, respectively. As discussed above, it was explained that Hf-GO could be reused for at least twelve times without obvious dropping in the catalytic performance.

S6. Activation effects of different temperatures on Hf-GO

The effect of isopropanol pretreatment temperatures on the activation effect was investigated. The fresh Hf-GO was treated with isopropanol at different temperatures for 2 h denoted by Hf-GO-Y (Y=25, 50, 70, 100, 120, 150, 170, 200 °C) and the catalyst activity were shown in Fig. S5, S6. As seen, compared with the fresh Hf-GO catalyst, the conversion of EL and GVL yield for Hf-GO-Y catalysts increased when the isopropanol pretreatment temperature increased from 25 °C to 150 °C. The activation effects became weaker when the pretreatment temperatures increased to 170 and 200 °C, but the activation effects still existed with higher conversion and yield compared to the fresh Hf-GO.

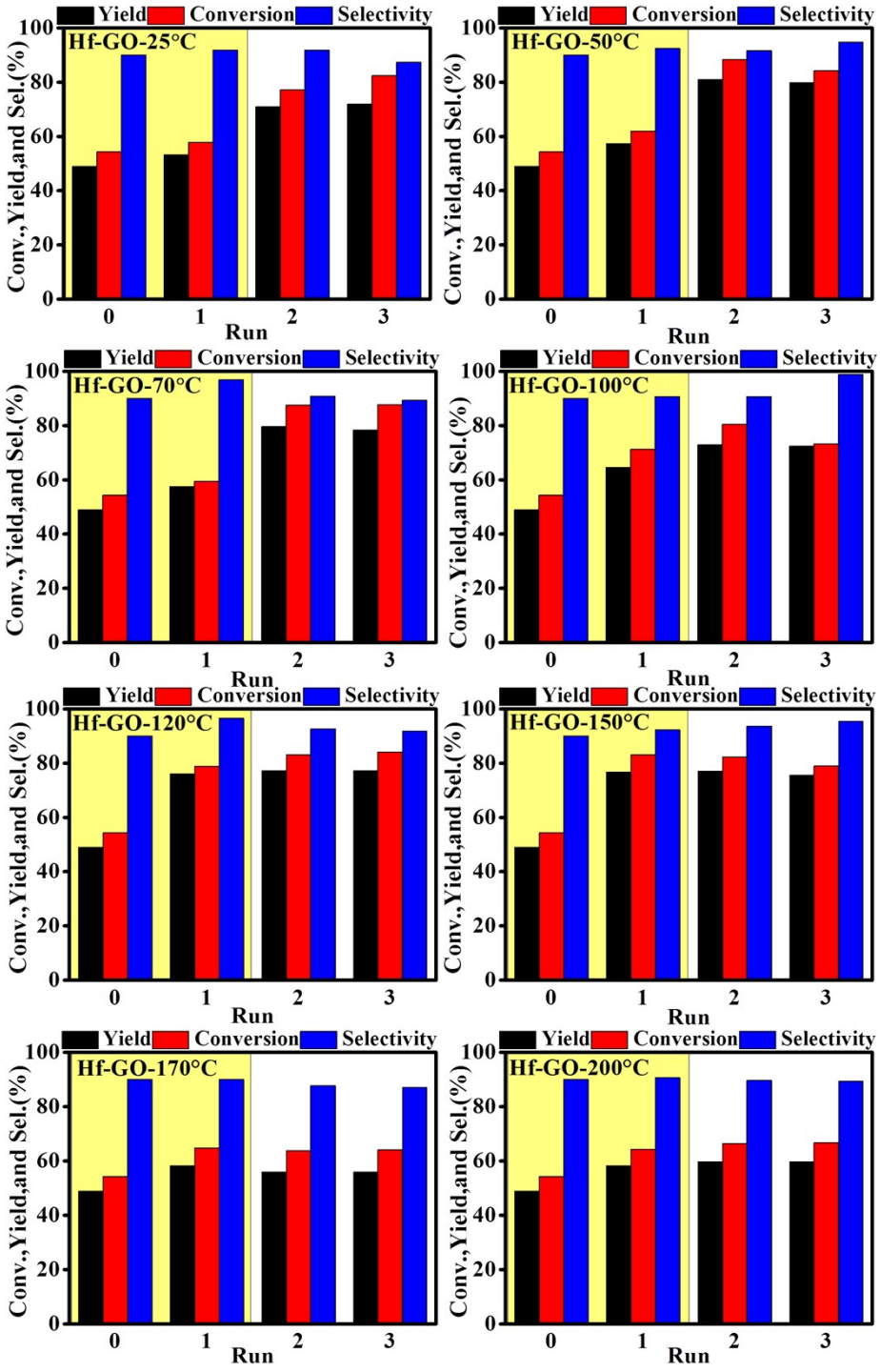

Fig. S5. Effects of pretreatment temperature on the activation effect of isopropanol on Hf-GO. Hf-GO-Y: Hf-GO catalyst pretreated by isopropanol under the temperature Y (Y= =25, 50, 70, 100, 120, 150, 170, and 200 °C). Run 0: the performance of the fresh Hf-GO catalyst without pretreatment. Run 1, 2, 3: the performance of Hf-GO-Y catalyst during three consequent uses. Reaction conditions: 1 mmol EL, 0.1 g catalyst (5 mol% Hf), 5 mL 2-PrOH, 150 °C, 2 h.

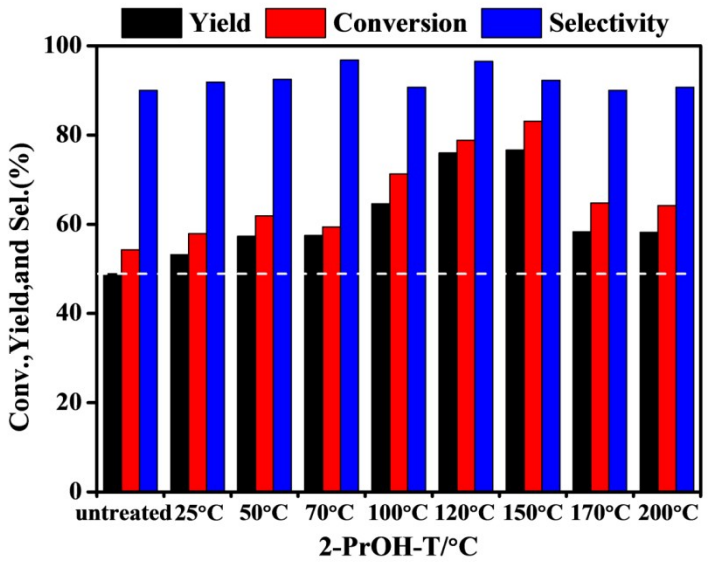

Fig. S6. Summarization of the effect of pretreatment temperature on the activation effect of isopropanol on Hf-GO. Reaction conditions: 1 mmol EL, 0.1 g catalyst (5 mol% Hf), 5 mL 2-PrOH, 150 °C, 2 h.

S7. Activation effects of different solvents

Fig. S7 and S8 showed the influences of alcohol type on Hf-GO. The fresh Hf-GO was treated with various alcohols at 150 °C for 2 h to give Hf-GO-X (X=MeOH, EtOH, nPrOH, nBuOH, nHeOH, nOcOH, iPrOH, sBuOH). It could be seen that all the alcohols had activation effects on Hf-GO compared to the fresh Hf-GO. Among MeOH, EtOH, nPrOH, nBuOH, nHeOH, nOcOH, iPrOH and sBuOH, the Hf-GO-iPrOH and Hf-GO-sBuOH were proved to give the most significant activation effects on Hf-GO. It seemed that the activation effects of the secondary alcohol were better than those of the primary alcohols (Fig. S8). Other solvents, including acetone, hexanone, and decane were also attempted to activate Hf-GO, but no obvious activation effects were observed (Fig. S9), which would be discussed in the

manuscript.

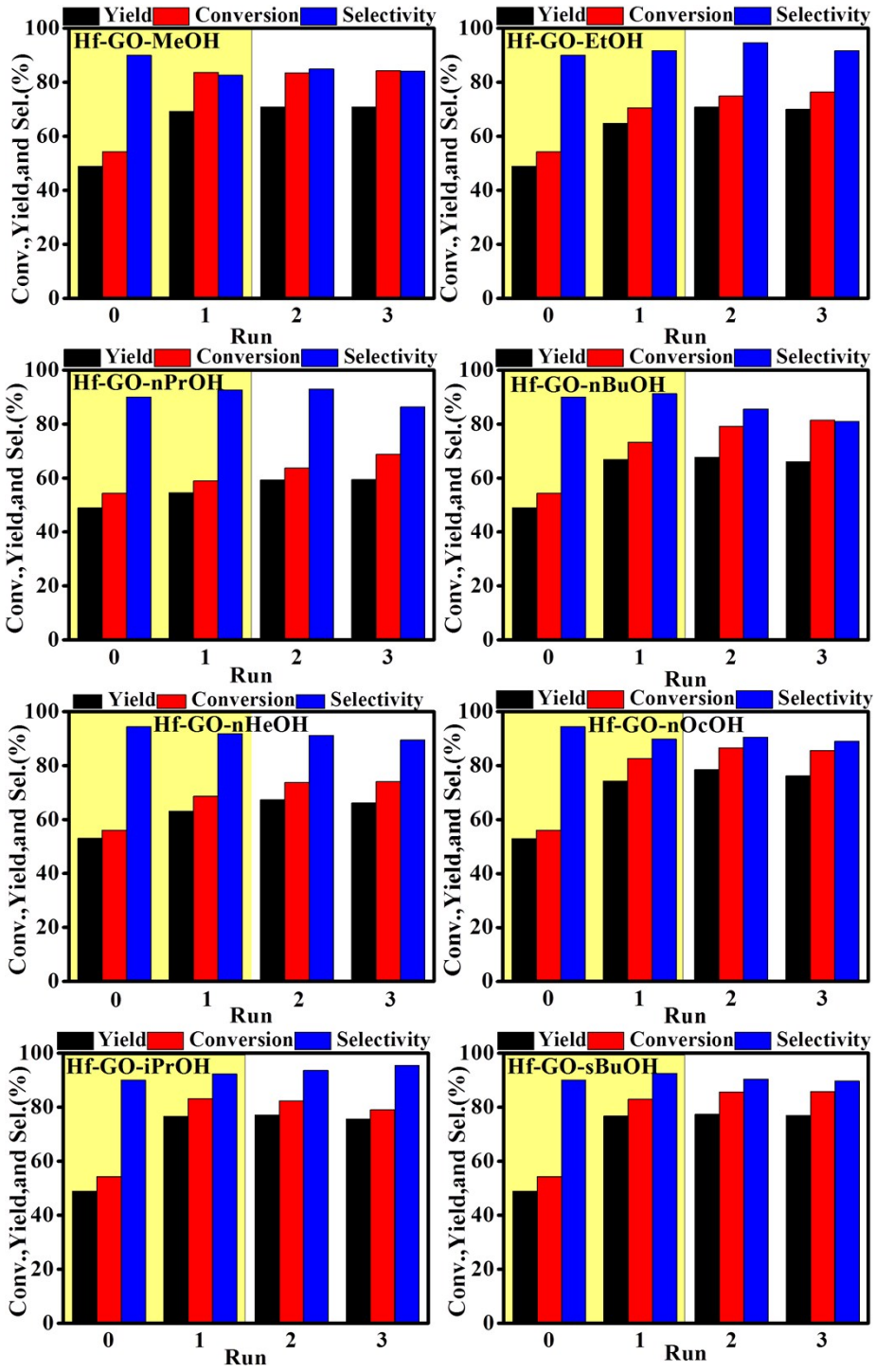

Fig. S7. Activation effects of different alcohols. Run 0: the performance of the fresh Hf-GO catalyst without isopropanol pretreatment. Run 1, 2, 3: the performances of Hf-GO-X catalyst (pretreated by alcohol X) during three consequent recycles. Reaction conditions: 1 mmol EL, 0.1 g catalyst (5 mol% Hf), 5 mL 2-PrOH, 150 °C, 2 h.

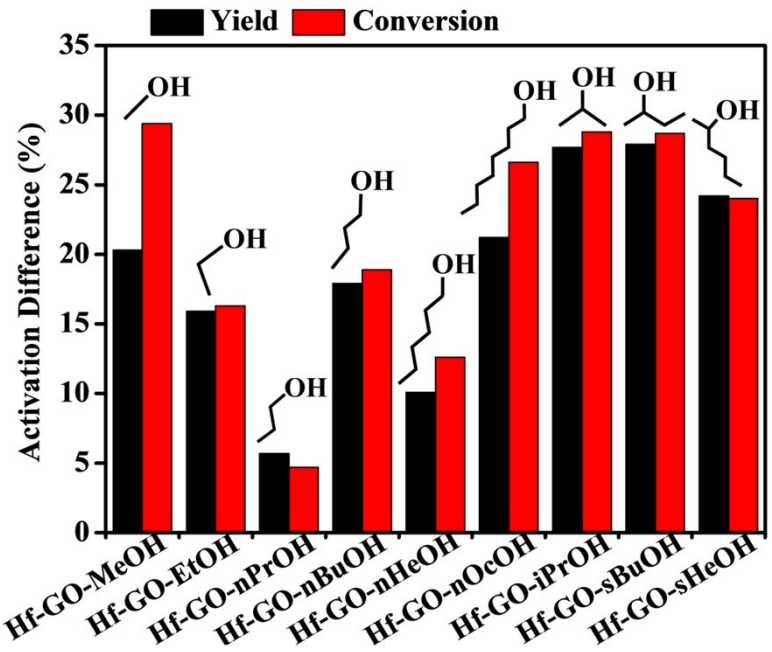

Fig. S8. Comparison of the activation effect of different alcohol types. The activation difference (%) in the y axis meant the differences of conversion and yield values for pretreated Hf-GO subtracted by those for Hf-GO without pretreatment.

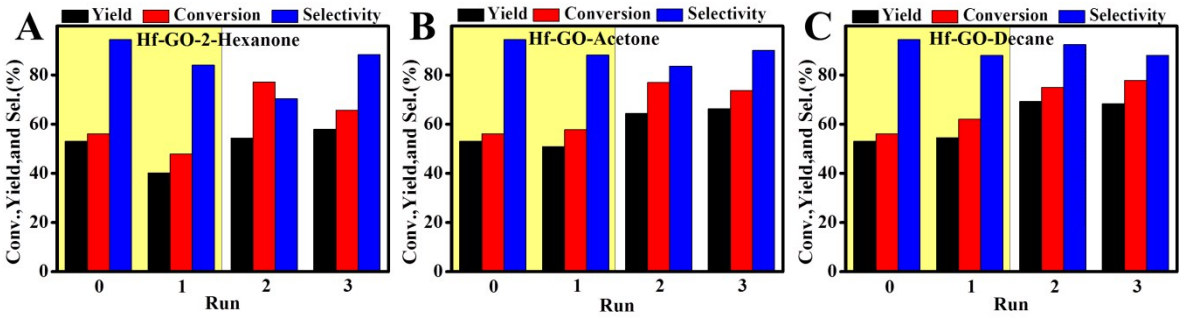

Fig. S9. Activation effect of hexanone (A), acetone (B), and decane (C). Run 0: the performance of the fresh Hf-GO catalyst without pretreatment. Run 1, 2, 3: the performance of the Hf-GO-X catalyst (pretreated by solvent X, X=acetone, hexanone, and decane) during three consequent cycles. Reaction conditions: 1 mmol EL, 0.1 g catalyst (5 mol% Hf), 5 mL 2-PrOH, 150 °C, 2 h.

S8. Characterization of the recycled and pretreated Hf-GO

The microscopic structures of the recovered and pretreated Hf-GO were characterized by SEM, TEM, EDS and SEM elemental mappings, and the results were shown in Fig. S10. It can be seen that the surface structure of the catalyst and distribution of Hf had no obvious change after use. Hf content was estimated to be approximately 11.87 *wt*% similar to that of the fresh Hf-GO. As shown in Fig. S11, the fresh catalyst had a diffraction peak of (001) at 2θ=10º (d=0.80 nm) but the peak was completely disappeared for the used catalyst. And the main broad peak of (002) changed from 21º (d=0.42 nm) to 24º (d=0.37 nm) for the used catalyst. The XRD patterns of the typical pretreated catalyst including Hf-GO-iPrOH, Hf-GO-DMF and Hf-GO-GVL catalysts had similar characteristic peak and structural properties like the used catalyst (Fig. S11, Table S3).

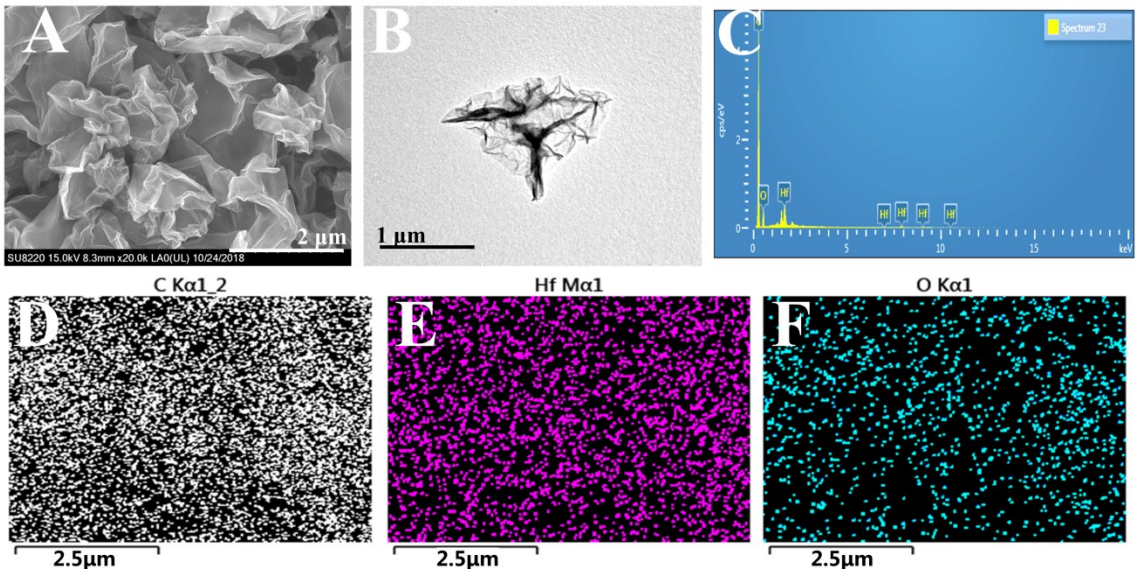

Fig. S10. (A) SEM image, (B) TEM image, (C) EDS, and (D, E, F) EDS-mapping of the Hf-GO-Used 12 times.

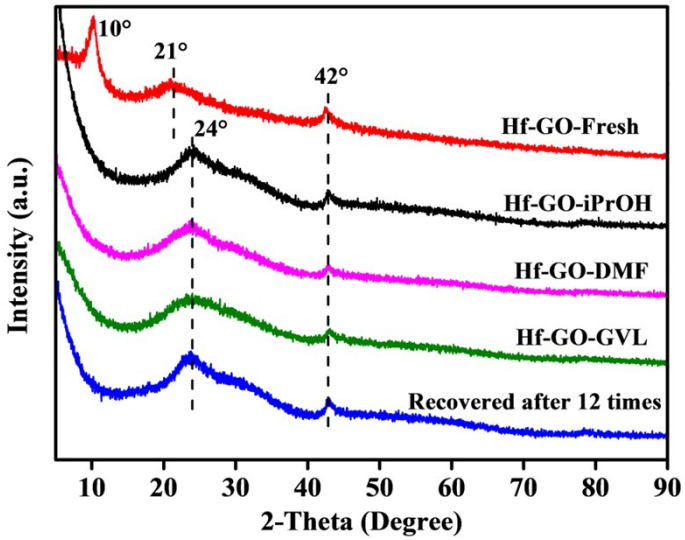

Fig. S11. XRD patterns of the recovered and pretreated catalysts.

Table S3. The *d*-spacing of main peaks of the GO, fresh, recovered, and pretreated catalysts by different solvents based on XRD patterns.

Sample	*d*-Spacing(nm)		
	001 Peak	002 Peak	010 Peak
GO	0.74	0.42	0.21
Hf-GO-Fresh	0.80	0.42	0.21
Hf-GO-iPrOH	-	0.37	0.21
Hf-GO-DMF	-	0.37	0.21
Hf-GO-GVL	-	0.37	0.21
Hf-GO-Used 12 times	-	0.37	0.21

From the Raman and XPS analysis (Fig. S12, S13, Tables S4, S5), no obvious changes were observed on either the shift of G band or D band in Raman spectra or the shift of peak XPS spectra, but the I_D/I_G ratio in Raman spectra showed obvious differences compared to the pristine Hf-GO. Element analysis validated that the pretreated Hf-GO-X catalysts had a decrease in the O content compared to the Hf-GO-Fresh. The intensity ratio of I_D/I_G increased from 1.00 for the pristine Hf-GO to 1.12 or 1.27 for other Hf-GO. This increase was regarded as the removal of DMF or partial oxygen functional groups in the GO sheets. TG showed that the weight losses for fresh Hf-GO were obviously higher than those of the recovered and pretreated Hf-GO (Fig. S14). These results further indicated that the pretreatment by solvents had no significant effects on the bulk structures but could affect the microstructures of Hf-GO. Meanwhile, these results also proved that Hf-GO was stable during recycling process.

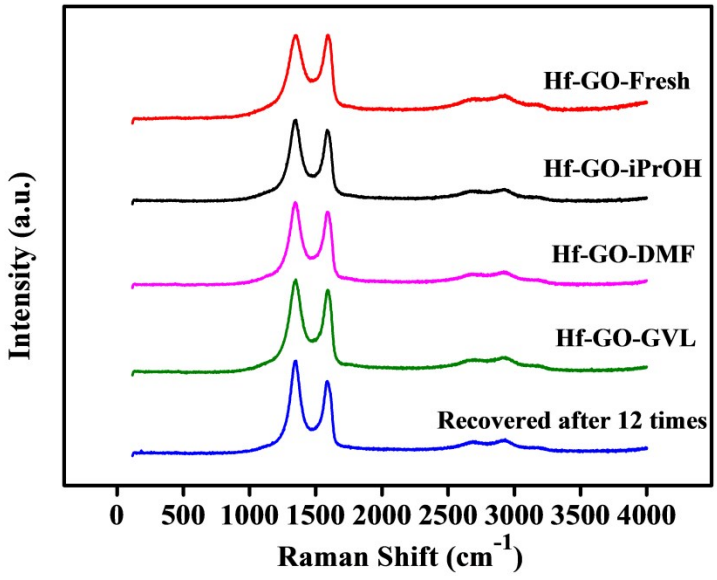

Fig. S12. Raman spectra of the fresh, recovered, and pretreated catalysts by different solvents.

Table S4. Raman data from the above Raman spectra.

Sample	Raman Shift (cm^{-1})		
	D Band	**G Band**	**I_D/I_G**
GO	1345	1596	0.94
Hf-GO-Fresh	1350	1589	1.00
Hf-GO-iPrOH	1350	1586	1.12
Hf-GO-DMF	1345	1586	1.12
Hf-GO-GVL	1345	1586	1.12
Hf-GO-Used 12 times	1350	1586	1.27

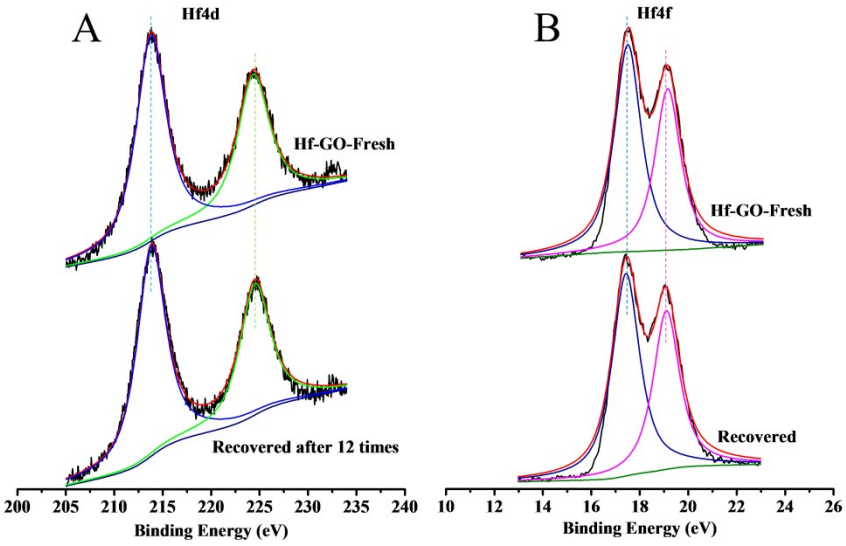

Fig. S13. Fitted spectra (A) Hf 4d and (B) Hf 4f peak in the XPS spectra of fresh and recovered after 12 times Hf-GO samples.

Table S5. Distribution of element species in GO, fresh Hf-GO, recovered Hf-GO samples from the fitting of the C 1s peaks by XPS.

E/eV	Carbon form	Content mol/% [a]		
		GO	Hf-GO	Recovered Hf-GO
284.8	C-C,C-H	50.43	64.98	79.44
286.7	C-O	24.79	22.74	14.03
287.2	C=O	22.39	7.82	3.16
288.8	O=C-O	2.39	4.46	3.36

[a] Obtained from the fitted peak area.

Table S6. Elemental contents of GO precursor and the obtained catalysts .

Entry	Sample	Element wt%				
		Hf[a]	C[b]	H[b]	O[b]	N[b]
1	GO		47.54	2.94	33.73	0.04
2	Hf-GO-Fresh	9.04	47.23	2.97	25.74	1.55
3	Hf-GO-iPrOH	11.94	62.52	2.12	9.77	0.97
4	Hf-GO-DMF	10.94	59.38	2.54	12.05	3.52
5	Hf-GO-Decane	11.08	63.34	2.47	13.03	0.67
6	Hf-GO-Acetone	10.60	64.35	2.35	13.60	0.40
7	Hf-GO-200 °C [c]	12.83	64.82	1.30	9.4	0.47

8	Hf-GO-Used 12 times	12.87	ND[e]	ND	ND	ND
9	Hf-GO-Fresh-150 °C dried[d]	ND	54.08	1.63	21.76	1.51
10	Hf-H_3BTC	45.46	17.13	2.15	18.18	0.18

[a] Measurements by Inductively coupled plasma atomic emission spectroscopy (ICP-AES). [b] Measurements by Elemental analysis (EA). [c] The fresh Hf-GO was treated with isopropanol at 200 °C for 2 h. [d] The fresh Hf-GO dried under vacuum conditions at 150 °C for 5 h. [e] ND: Not detected.

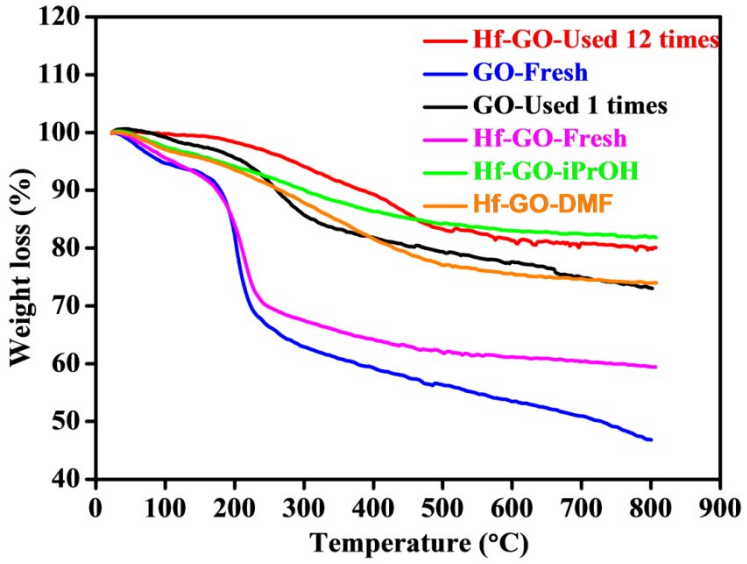

Fig. S14. TG curves of GO and Hf-GO catalysts with different treatment.

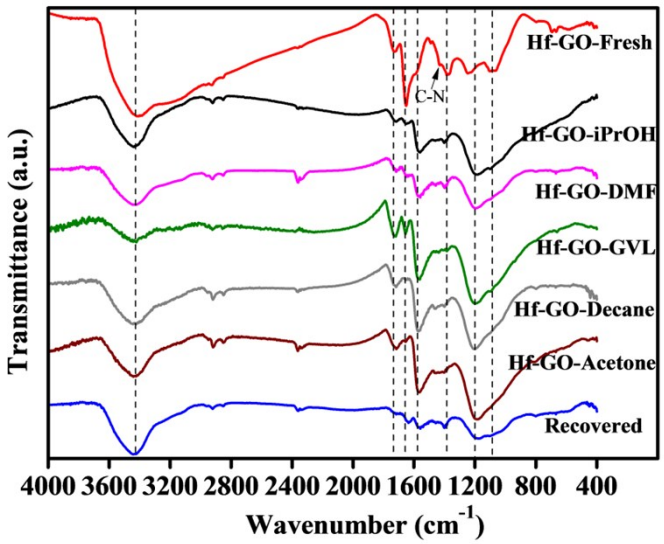

Fig. S15. FTIR spectra of the fresh, recovered, and pretreated Hf-GO catalysts by different solvents.

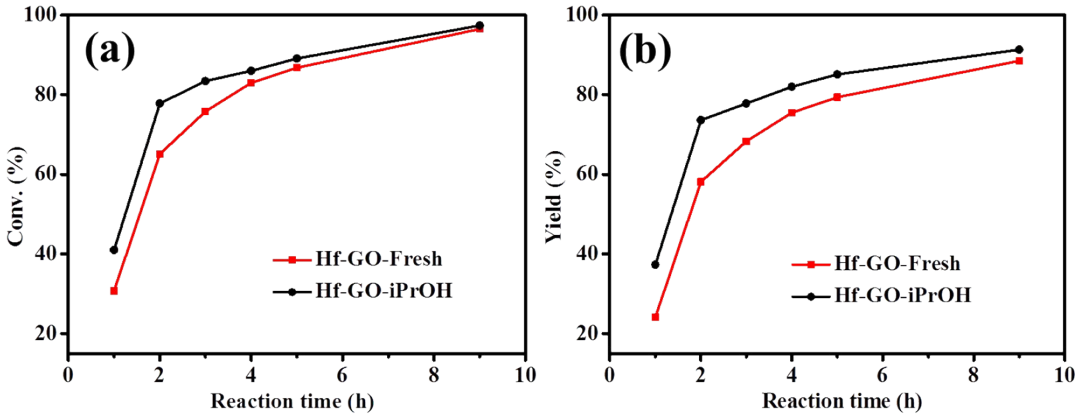

Fig. S16. Time-profiles of Hf-GO freshly prepared in DMF (Hf-GO-fresh) and Hf-GO pretreated by isopropanol (Hf-GO-iPrOH). Reaction conditions: 1 mmol EL, 0.1 g catalyst, 5 mL 2-PrOH , reaction temperature 150 °C, and the required reaction time.

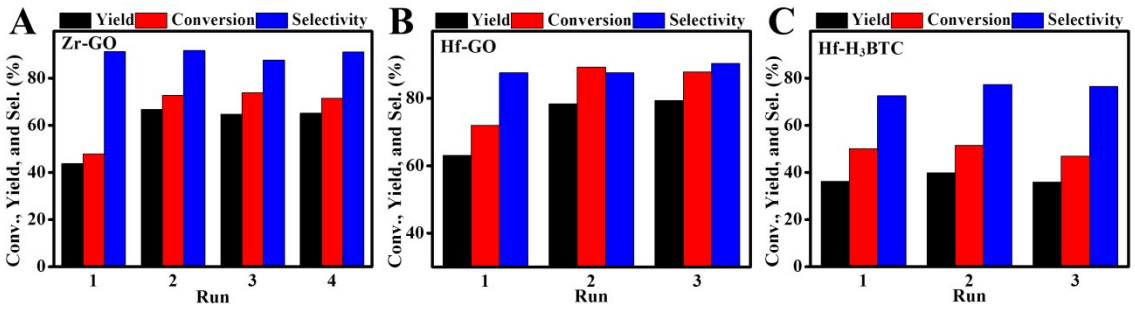

Fig. S17. Activation effects of isopropanol on different catalysts. (A) Zr-GO, (B) Hf-GO, and (C) Hf-H_3BTC. Reaction conditions: (A) 1 mmol EL, 0.1 g catalyst, 5 mL 2-PrOH, 150 °C, 2 h. (B) 1 mmol FF, 0.1 g catalyst, 5 mL 2-PrOH, 70 °C, 2 h. (C) 1 mmol EL, 0.1 g catalyst, 5 mL 2-PrOH, 130 °C, 2 h.

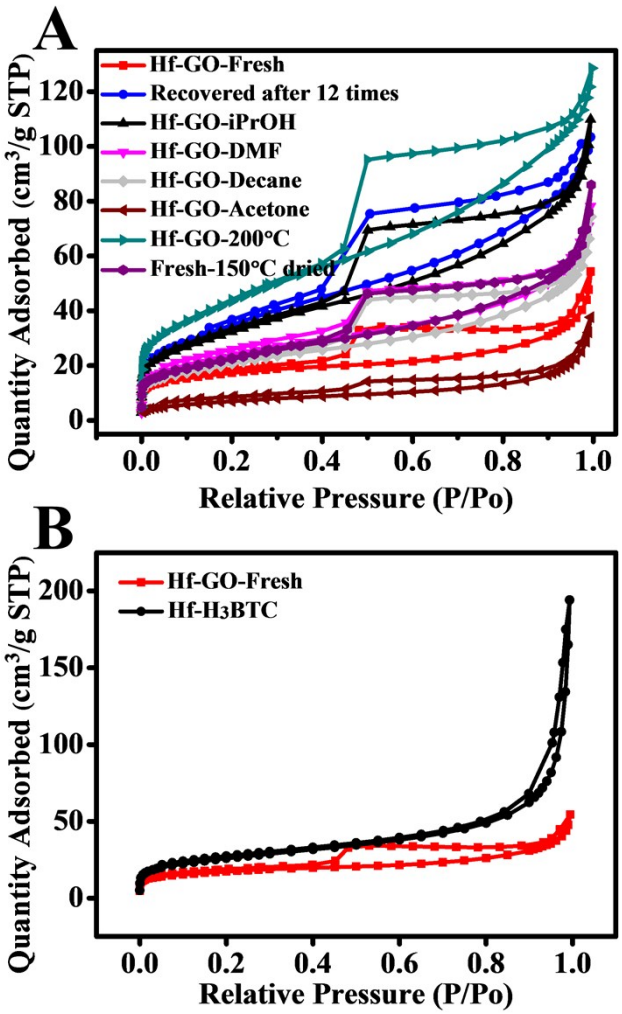

Fig. S18. N_2 adsorption-desorption isotherms of different Hf-GO catalysts (A) and comparison of Hf-GO-fresh with Hf-H_3BTC (B).

Table S7. Comparison of pore features for the investigated catalysts and GO precursor.

Sample	S_{BET} (m^2/g)[a]	V_t (cm^3/g)[b]	V_{mic} (cm^3/g)[b]	V_{mes} (cm^3/g)[b]	D_{mea} (nm)[c]
GO	98.8	0.13	0.02	0.11	4.6
Hf-GO-Fresh	61.8	0.08	0.01	0.07	6.1
Hf-GO-iPrOH	113.9	0.17	0.001	0.169	5.3
Hf-GO-Used 12 times	127.4	0.16	0.03	0.13	4.4
Hf-GO-DMF	83.4	0.12	0.002	0.118	5.3
Hf-GO-Decane	70.0	0.12	0.001	0.119	5.8
Hf-GO-Acetone	26.0	0.06	0.002	0.058	8.7
Hf-GO-200 °C [d]	155.3	0.20	0.01	0.19	4.5
Hf-GO-F-150°C dried [e]	80.3	0.13	0.004	0.126	6.1
Hf-H_3BTC	93.3	0.30	0.01	0.29	17.6

[a] S_{BET}: Brunauer-Emmett-Teller (BET) specific surface area.

[b] Volume of pores was estimated from single point adsorption total pore volume of pores.

[c] D_{mea}: average pore size was estimated from the D-H desorption average pore diameter.

[d] The fresh Hf-GO was treated with isopropanol at 200 °C for 2 h.

[e] The fresh Hf-GO dried under vacuum conditions at 150 °C for 5 h.

Table S8. The surface contents of Hf in Hf-GO pretreated by different solvents.

Entry	Sample	Hf Atomic ratio% [a]
1	Hf-GO-iPrOH	0.80
2	Hf-GO-DMF	0.73
3	Hf-GO-GVL	0.81

[a] Calculated by XPS data.

References

1. Z. H. Xiao, H. C. Zhou, J. M. Hao, H. L. Hong, Y. M. Song, R. X. He, K. D. Zhi and Q. S. Liu, *Fuel*, 2017, **193**, 322-330.
2. J. L. Song, L. Q. Wu, B. W. Zhou, H. C. Zhou, H. L. Fan, Y. Y. Yang, Q. L. Meng and B. X. Han, *Green Chem.*, 2015, **17**, 1626-1632.
3. L. Peng, J. L. Zhang, J. S. Li, B. X. Han, Z. M. Xue and G. Y. Yang, *Chem. Commun.*, 2012, **48**, 8688-8690.
4. H. Li, Y. Li, Z. Fang and R. L. Smith, *Catal. Today*, 2019, **319**, 84-92.
5. D. Mondal, J. P. Chaudhary, M. Sharma and K. Prasad, *RSC Adv.*, 2014, **4**, 29834-29839.
6. R. Y. N. Gengler, D. S. Badali, D. F. Zhang, K. Dimos, K. Spyrou, D. Gournis and R. J. D. Miller, *Nat. Commun.*, 2013, **4**, 2560.
7. H. Li, T. Yang and Z. Fang, *Appl. Catal. B-Environ.*, 2018, **227**, 79-89.
8. K. B. Lausund and O. Nilsen, *Nat. Commun.*, 2016, **7**, 13578.
9. J. Cheng, J. Wang, X. Wang and H. Wang, *Ceram. Int.*, 2017, **43**, 7159-7165.
10. M. Acik, G. Lee, C. Mattevi, M. Chhowalla, K. Cho and Y. J. Chabal, *Nat. Mater.*, 2010, **9**, 840-845.
11. B. B. Zhang, J. X. Hao, Y. F. Sha, H. C. Zhou, K. L. Yang, Y. M. Song, Y. P. Ban, R. X. He and Q. S. Liu, *Fuel*, 2018, **217**, 122-130.
12. L. Lu, V. Sahajwalla, C. Kong and D. Harris, *Carbon*, 2001, **39**, 1821-1833.

13. G. Lv, H. Wang, Y. Yang, X. Li, T. Deng, C. Chen, Y. Zhu and X. Hou, *Catal. Sci. Technol.*, 2016, **6**, 2377-2386.
14. G. Lv, H. Wang, Y. Yang, T. Deng, C. Chen, Y. Zhu and X. Hou, *Acs Catal.*, 2015, **5**, 5636-5646.
15. O. Akhavan, *Acs Nano*, 2010, **4**, 4174-4180.
16. P. P. Upare, J.-W. Yoon, M. Y. Kim, H.-Y. Kang, D. W. Hwang, Y. K. Hwang, H. H. Kung and J.-S. Chang, *Green Chem.*, 2013, **15**, 2935.
17. D. Roy, E. Angeles-Tactay, R. J. C. Brown, S. J. Spencer, T. Fry, T. A. Dunton, T. Young and M. J. T. Milton, *Chem. Phys. Lett.*, 2008, **465**, 254-257.